3-D vertical cable processing using EOM

Carlos Rodriguez-Suarez, John C. Bancroft, Yong Xu and Robert R. Stewart

ABSTRACT

Three-dimensional seismic data using vertical cables was modeled and processed using equivalent offset migration (EOM), a pre-stack time migration method developed by CREWES.

The data was generated using 3-D ray tracing over a geological model obtained from seismic interpretation performed on a giant Brazilian offshore oil field. Velocity variations in three directions were obtained from 3-D seismic data acquired over the field.

The results show EOM is capable of handling a very large data set, but some noise created by the method is not attenuated after stacking.

INTRODUCTION

The advantages and characteristics of the vertical cable technique were outlined by Rodriguez-Suarez and Stewart (1998) in last year's CREWES Research Report. Equivalent offset migration (EOM) is a Kirchhoff pre-stack time migration developed by CREWES, which uses the concept of common scatter points (CSP). The use of 3-D EOM for vertical receiver array processing has been presented by Bancroft and Xu (1998). The authors processed a 3D-VSP in the Blackfoot area. Since then, the use of EOM for vertical receiver arrays on data from numerical modeling of increasing complexity (*e.g.* constant velocity, layered and linear increasing velocity media) and size has been analyzed.

Some acquisition issues, such as seismic resolution, aperture, and receiver cable distances, are discussed in this year's CREWES Research Report by Bancroft *et al.* (1999).

In this paper, we present the use of EOM to process a large volume of 3-D data. The data set used was generated by three-dimensional ray tracing over a geological model obtained from seismic interpretation on a giant Brazilian offshore oil field. Velocities for the sedimentary layers were obtained from the velocity cube used in the processing of the seismic data over the oil field.

We show that EOM is capable of processing a very large amount of data, giving a good seismic response in a reasonable amount of computer time, while using a simple processing flow. However, our results also show that strong noise may be created in the process.

GEOLOGICAL MODEL AND RAY TRACING

The geological model (Figure 1) is based on the 3-D seismic interpretation of a giant deep-water oil field, offshore Brazil. The oil field is located in a continental passive margin basin, developed in the late Mesozoic during the separation of what are now the continents of South America and Africa.

The sediments are mainly sands and shales deposited in a shallow to deep-water environment, with some associated limestone. The reservoir is a deep water unconsolidated sandstone turbidite.

Four interfaces were used in the modeling: sea bottom, Miocene, Oligocene, and a reservoir target. Maximum depth is 4 km and area extension, 11.5 km (E-W direction) by 9 km (N-S direction).

Lateral velocity variations were obtained through conversion of seismic processing velocities to interval velocities using the Dix equation. For each X,Y position, the velocity was constant inside each layer. The processing velocity grid was resampled from 500 x 500 m to 1000 x 1000 m, to simplify (and increase the speed of) the ray tracing.

Quality factors (Q) varying from 30 (for shallow sediments) to 80 (deepest layer), common in these lithologies, were used in the model. Density was obtained using Gardner's relationship (except for water, where a constant value of 1.05 was applied). High Poisson's ratios – 0.4 for the sediment below the water, and 0.3 for the deepest layer – were used to obtain shear wave velocities due to the poor consolidation of the sediments.

Ten cables, laid in a grid approximately 2 x 3 km, were initially used. The shot point grid had to be relatively large – 100 x 100 m – due to the long ray tracing time. The maximum source-receiver offset was between 6,000 and 8,000 m. Each cable had 16 hydrophones, with a 30 m depth interval, from 30 to 480 m. Figure 2 shows a map view of the shot point distribution for some cables together with their positioning.

For the ray tracing, the numerical modeling program GX 3D-VSP^{TM}, from GX Technology, was used. The algorithm is really 3-D, so reflections out of the source-receiver vertical plane are also considered. No multiple reflections or downgoing reflected energy from the sea surface were considered for the ray tracing. Only the P-P wave field was recorded.

The ray tracing method used by 3D-VSP^{TM} is presented in Pereyra (1988). It consists of a global (bending) two-point ray tracing technique, which works in complex media. A simple shooting algorithm provides starting rays for the two-point module, which then uses receiver continuation to generate coherent ray families. The representation of many geological unconformities (e.g., normal and reverse faults, pinchouts, and salt domes) is possible with this method.

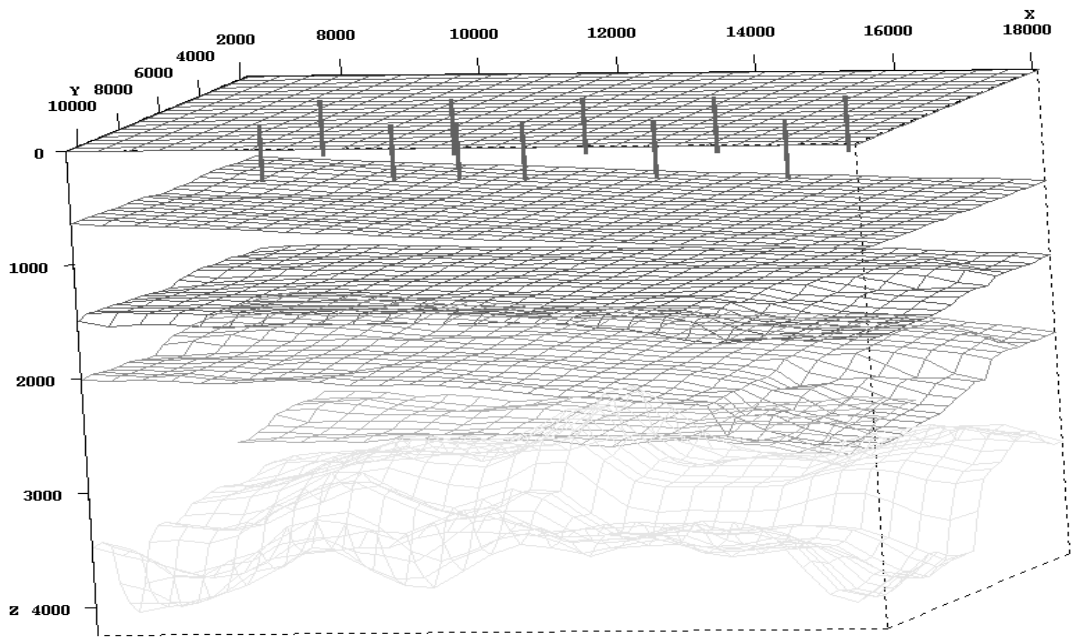

Figure 1 – 3-D view of the geologic model. From top to bottom: sea level, sea bottom, Miocene, Oligocene, Reservoir (smaller horizon), and Cretaceous. Note that the Cretaceous, gently dipping to east (increasing X), is the most structured interface. Most cables are also shown. Distance in meters.

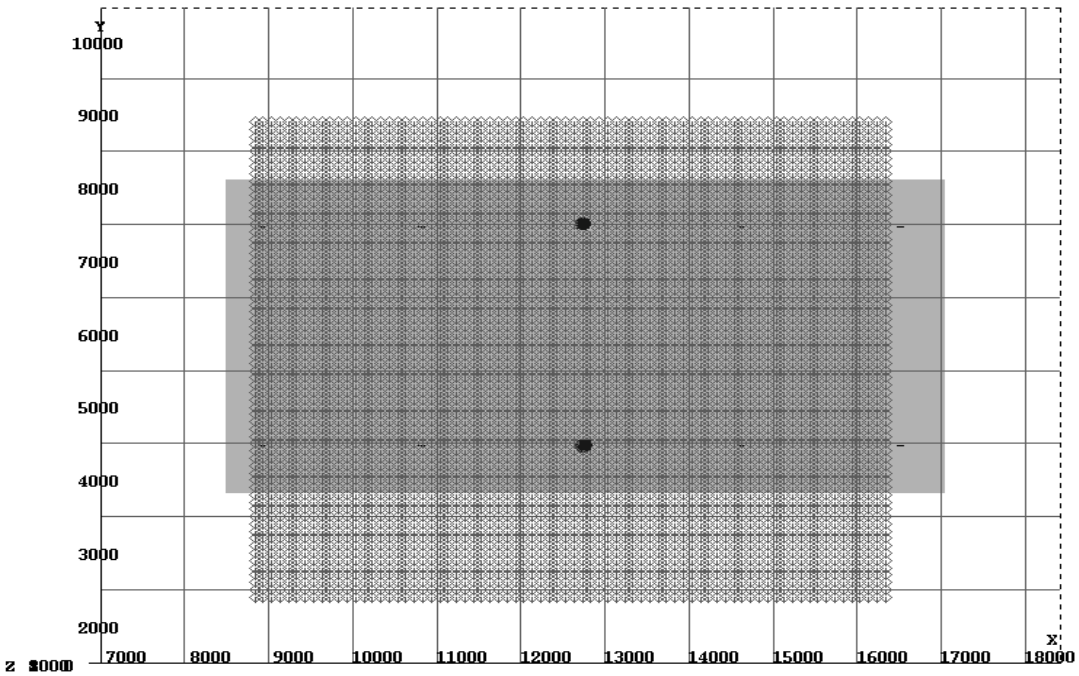

Figure 2 – Map view of the shot point grid (the rectangle from approximately 9000 to 16500 along X and 3000 to 9500 along Y) and reservoir (the rectangle from approximately 8500 to 17000 along X and 4300 to 8500 along Y). This shot point grid was used for the cables indicated by black circles. Distances in meters.

The most important ray tracing parameters (GX, 1994, 1997) used in GX 3D-VSP^{TM} were:

- *propagation mode*: P-wave only

- *ray shooting mode*: 2-point continuation. Once a shot-to-receiver path has been found, the other receiver reflections are obtained using receiver continuation; increasing the speed of the ray tracing

- *search control*: a value of 2 was used for primary, inline, and crossline. These parameters – which vary from 1 to 100 – specify the density of searching used during ray tracing. The *primary* field controls how dense the search is on the horizon during the first and final passes of ray tracing. It should increase according to the model complexity (GX, 1997). *Inline* (along the longest axis of receiver pattern) and *crossline* (perpendicular to inline) control how searching is performed on the receiver array. The larger they are, the more precise (and slower) the ray tracing procedure. A technical support geophysicist at GX, Ms. Susan Collins, recommended the value of 2.

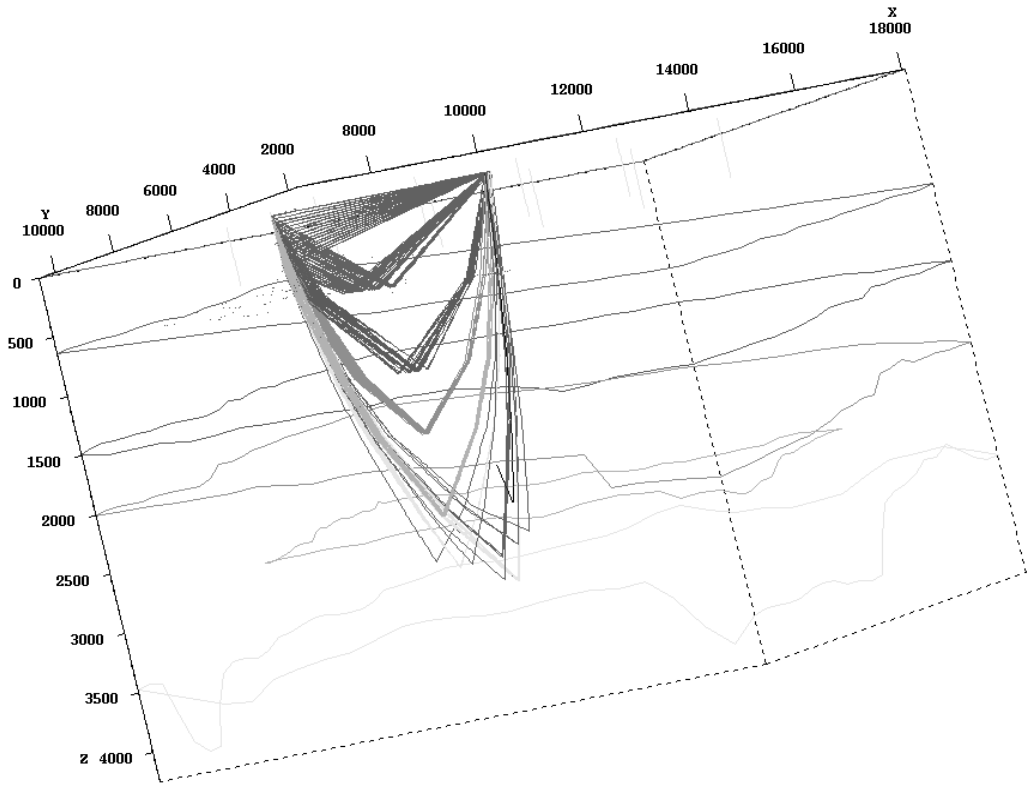

Figure 3 – Rays propagating through the model.

The ray tracing amplitudes are obtained by Zoeppritz equations, as presented by Young and Braile (1976). The reflection coefficients were convolved with a 30 Hz zero-phase Ricker wavelet.

Using a Sun Ultra 10/400 MHz workstation, the computer time for the ray tracing varied from five to seven days. The whole dataset had around 50,000 shot points and 800,000 traces.

Figure 3 shows some rays propagated in the model. Figure 4 shows some examples of shot gathers from the modeling.

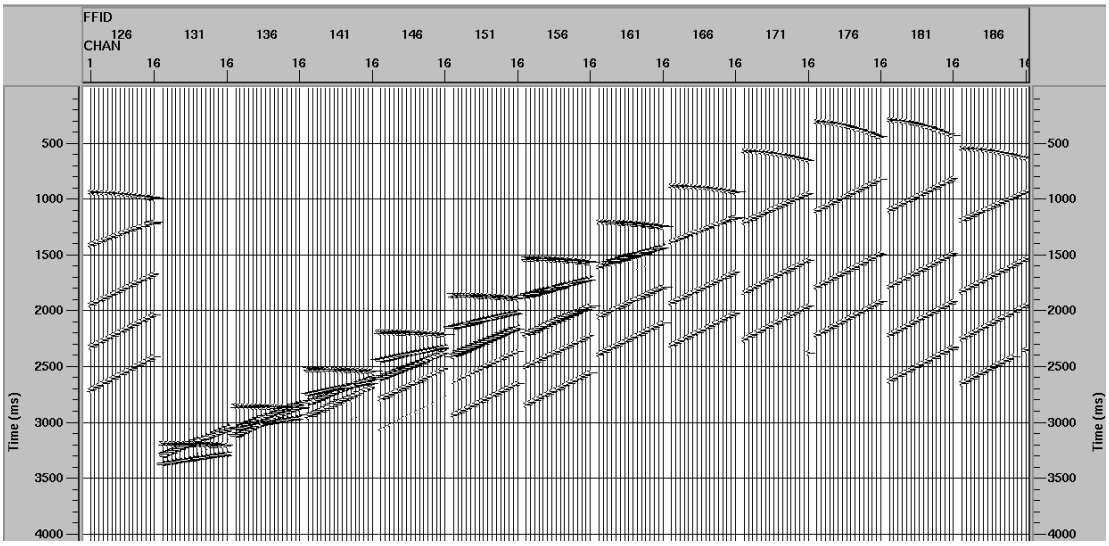

Figure 4 – Numerical model shot gathers. The events (top to bottom) are direct waves and reflections from sea bottom, Miocene, Oligocene, and reservoir.

DATA PROCESSING RESULTS

The Seismic Unix (SU) suite of algorithms was used at all stages of the data processing, except for velocity analysis, some displays, and the EOM. A velocity function, obtained from averaging the model interval velocity values, was used to obtain initial values for the pre-stack migration. After the migration, velocity analysis was done by semblance using ProMAX. The velocity functions from the second analysis were used for stacking, to give the final processing result. All velocity cubes were converted to two-dimensional grids.

Necessary static corrections due to receiver depth (Bancroft and Xu, 1998) are easier to perform on marine than land data, as the velocity can be obtained with accuracy and considered as constant. A practical problem of determining exact receiver depth and position determination remains, though this is not the case for numerical model data.

Although SU is a 2-D package, EOM runs in a 3-D mode. This means that to obtain the final amplitude of a single sample *all* available data is used. Output from EOM can be a single 2-D line, in any desired direction, or a group of several parallel 2-D lines, with any distance between them.

The most important parameters to be defined by the user are the bin spacing in common scatter point (CSP) gathers and the number of bins in each gather (Bancroft

and Xu, 1998). Bin spacing usually equals half the shot point distance. The number of bins per gather determines the maximum aperture, so that the larger the number, the more precise the method becomes, although at the expense of more computer time. A value equal to the maximum depth of interest is often a good guess.

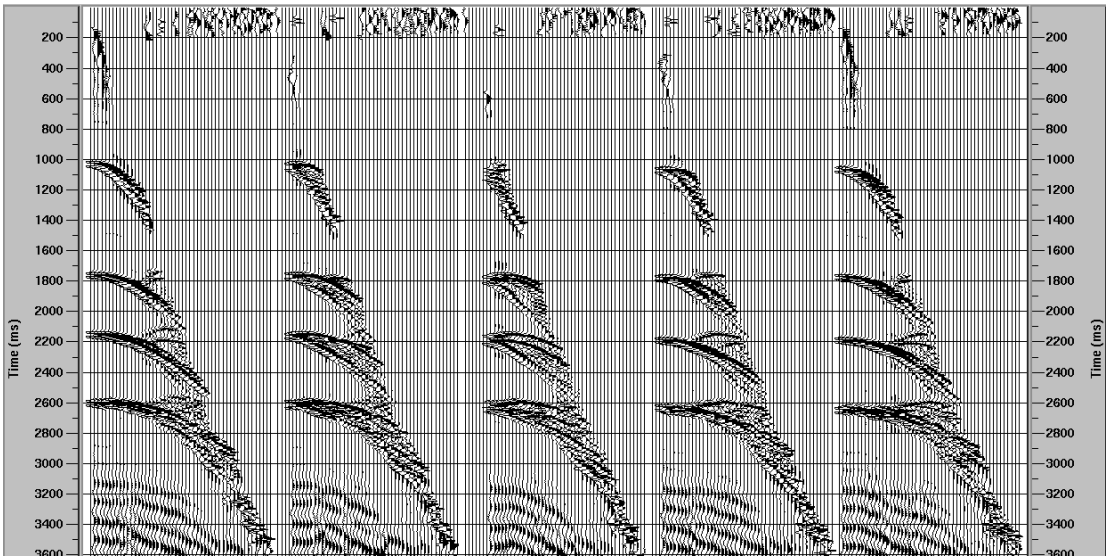

Figure 5 – Common scatter point (CSP) gathers after EOM, without NMO correction. After NMO correction and stack, most (but not all) diffuse energy around hyperbolic reflections will vanish. Noise above 200 ms and below 3400 ms is due to display gain.

Figure 5 shows some CSP gathers after EOM. We can see reflections with close to hyperbolic behavior and, around them, some diffuse energy. After NMO correction and stacking, most of this diffuse energy – but not all – will vanish. The presence of this energy in CSP gathers may be due to 1) poor velocity analysis, and/or 2) bad processing parameter choice, and/or 3) indicates that the method needs some additional refinements. The remaining diffuse energy, not attenuated during NMO and stack, appears in the final stacked section as strong amplitude noise, as shown in Figure 6.

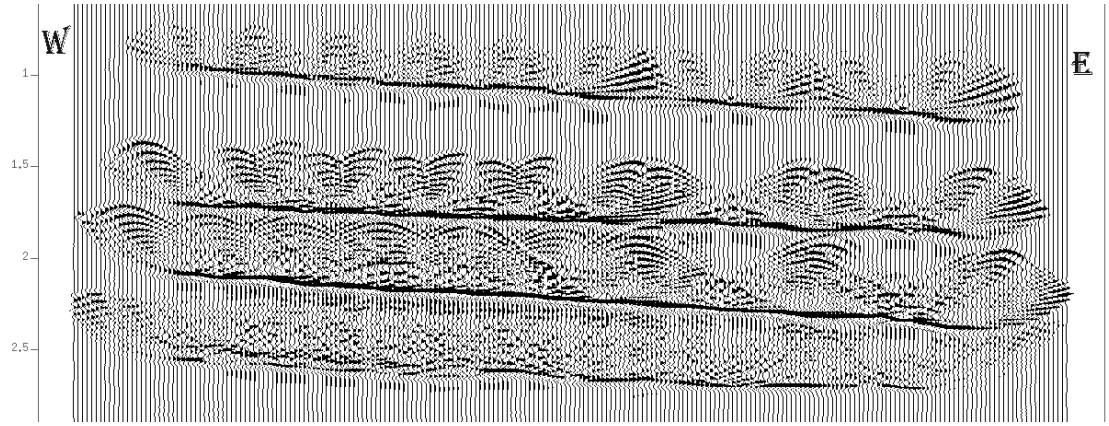

Figure 6 – Stacked section after EOM. Noise is caused by diffuse energy generated during EOM that was not attenuated with NMO correction and stack.

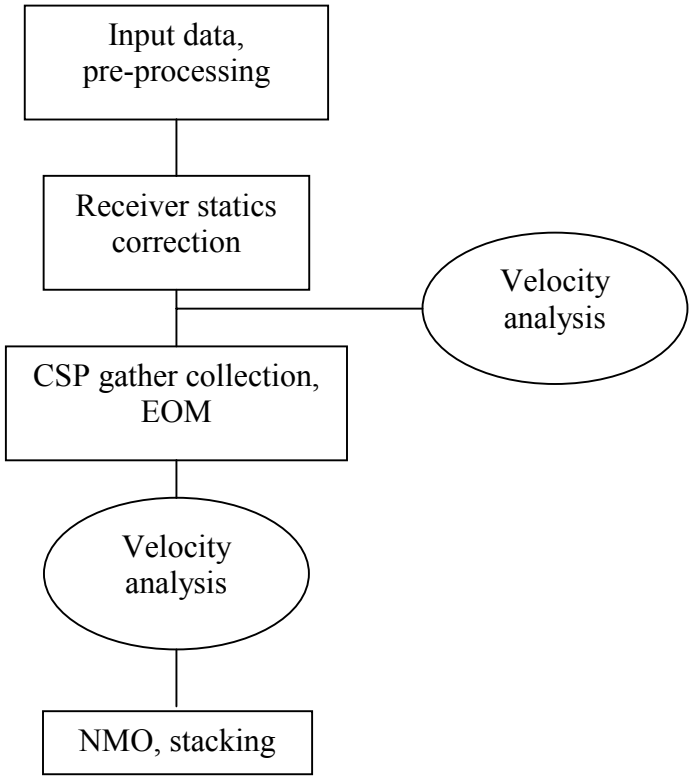

Figure 7 – Vertical cable processing flow using EOM. The receiver statics correction step may be difficult and time consuming for real data.

We believe the discontinuity in the deepest event on Figure 6 is caused by poor velocity analysis.

Figure 7 presents a general flow for vertical cable processing using EOM.

CONCLUSIONS

Equivalent offset migration (EOM) was capable of imaging a very large data set in a reasonable processing time. Some issues regarding noise generation during the EOM process remain to be addressed.

The EOM algorithm used for these results was designed to verify the kinematics. Improved amplitude scaling of the CSP gathers and tapering of the NMO correction will help to reduce the noise. This application of EOM is a Kirchhoff prestack time migration, and illustrates the quality that can be obtained with the Kirchhoff method. The CSP gathers provide visual detail of all the input energy that contributes to the final migration. Various implementations of the Kirchhoff algorithm will vary in amplitude scaling and filtering; however, the kinematics should remain similar.

ACKNOWLEDGEMENTS

We thank Xinxiang Li for his frequent, friendly advice, and Ms. Susan Collins (GX Technology) for technical support in using GX 3D-VSP™. Appreciation also to Henry Bland for his systems support at CREWES.

REFERENCES

Bancroft, J.C. and Xu, Y., 1998, Equivalent offset migration for vertical receiver arrays, CREWES Research Report, Vol. 10, Ch. 11.

Bancroft, J.C., Rodriguez-Suarez, C. and Xu, Y, 1999, Resolution of seismic data acquired with vertical receiver arrays, CREWES Research Report, this volume.

GX Technology, 1994. 3D-VSP™ User Guide: Release 2.0 Edition, November 1994.

GX Technology, 1997. A guide to 3D-VSP™ Seismic Simulation: Release 4.2, March 1997.

Pereyra, V., 1988, Two-point ray tracing in complex 3-D media: Presented at the 58th SEG Meeting, SI 5.6, p. 1056-1060.

Rodriguez-Suarez, C. and Stewart, R.R., 1998, Survey design for vertical cable seismic acquisition, CREWES Research Report, Vol. 10, Ch. 6.

Young, G.B. and Braile, L.W., 1976, A computer program for the application of Zoeppritz's amplitude equations and Knott's energy equations, Bull. Of Seismological Soc. of America, p. 1881-1885.